

# Bifurcations of self-similar solutions for reversing interfaces in the slow diffusion equation with strong absorption

J M Foster<sup>1</sup>, P Gysbers<sup>2,3</sup>, J R King<sup>4</sup> and D E Pelinovsky<sup>5</sup> 

<sup>1</sup> Department of Mathematics, University of Portsmouth, Portsmouth, PO1 2UP, United Kingdom

<sup>2</sup> Department of Physics & Astronomy, University of British Columbia, Vancouver, BC V6T 1Z1, Canada

<sup>3</sup> TRIUMF, Vancouver, BC V6T 2A3, Canada

<sup>4</sup> School of Mathematical Sciences, Nottingham University, Nottingham, NG7 2RD, United Kingdom

<sup>5</sup> Department of Mathematics & Statistics, McMaster University, Hamilton ON, L8S 4K1, Canada

E-mail: [jamie.foster@port.ac.uk](mailto:jamie.foster@port.ac.uk)

Received 1 February 2018, revised 3 July 2018

Accepted for publication 12 July 2018

Published 31 August 2018



CrossMark

Recommended by Professor Michael Jeffrey Ward

## Abstract

Bifurcations of self-similar solutions for reversing interfaces are studied in the slow diffusion equation with strong absorption. The self-similar solutions bifurcate from the time-independent solutions for standing interfaces. We show that such bifurcations occur at particular points in parameter space (characterizing the exponents in the diffusion and absorption terms) where the confluent hypergeometric functions satisfying Kummer's differential equation truncate to finite polynomials. A two-scale asymptotic method is employed to obtain the local dependencies of the self-similar reversing interfaces near the bifurcation points. The asymptotic results are shown to be in excellent agreement with numerical approximations of the self-similar solutions.

Keywords: slow diffusion, strong absorption, self-similar solutions, reversing interface, bifurcations, Kummer's differential equation, matched asymptotic expansions

Mathematics Subject Classification numbers: 35G31, 35R35, 35C06, 35C20, 35B40, 37G10

(Some figures may appear in colour only in the online journal)

### 1. Introduction

We address reversing interfaces in the following slow diffusion equation with strong absorption

$$\frac{\partial h}{\partial t} = \frac{\partial}{\partial x} \left( h^m \frac{\partial h}{\partial x} \right) - h^n, \tag{1.1}$$

where  $h(x, t)$  is a positive function on a compact support, e.g. a concentration of some species, and  $x$  and  $t$  denote space and time, respectively. Restricting the exponents to the ranges  $m > 0$  and  $n < 1$  limits our interest to the case of slow diffusion [15] and strong absorption [16, 18, 19], respectively. The restriction  $m > 0$  implies that the edges of the compact support propagate with a finite speed [9], whilst for  $n < 1$  compactly supported solutions go extinct in a finite time [5]. These two results suggest that, for certain choices of initial data which lead to an initial expansion of the compact support, reversing of interfaces can occur. Here, we use the term ‘reversing of interfaces’ to describe scenarios in which an advancing interface gives way to a receding interface; the term ‘anti-reversing’ of an interface describes the converse, i.e. a receding interface giving way to an advancing one, see figure 1. Such scenarios have been examined in this range of exponents previously in [7, 8]. For the limiting case when  $m + n = 1$  it has been shown, in [10], that solutions can exhibit reversing interfaces but cannot display a ‘waiting time’ where an interface remains static for some finite time and then begins to move. These ‘waiting-time’ solutions have also been studied for the slow diffusion equation but in absence of absorption in [17, 21]. The behaviour of solutions local to the extinction time has also been examined in the limiting case when  $m + n = 1$  in [11, 12] and in the general case  $m > 0$  and  $n < 1$  in [6].

The slow diffusion equation with strong absorption, (1.1), is relevant in a wide variety of different physical processes and can be used as a model for: (i) the slow spreading of a slender viscous film over a horizontal plate subject to the action of gravity and a constant evaporation rate [2] (when  $m = 3$  and  $n = 0$ ); (ii) the dispersion of a biological population subject to a constant death-rate [14] (when  $m = 2$  and  $n = 0$ ); (iii) nonlinear heat conduction along a rod with a constant rate of heat loss [15] (when  $m = 4$  and  $n = 0$ ), and; (iv) fluid flows in porous media with a drainage rate driven by gravity or background flows [3, 23] (when  $m = 1$  and  $n = 0$ ).

Let us denote the location of the left interface by  $x = s(t)$ . It was proven in [5] that compact initial data with a single maximum generates a compact solution in a simply-connected region for all time before the compact support shrinks to a point. If  $m > 0$ ,  $0 < n < 1$ , and  $m + n > 1$ , it was proved in [9] that the position of the interface,  $s(t)$ , is a Lipschitz continuous function of time. By invoking mass conservation at the interface, it was also shown that  $s(t)$  satisfies the following interface equation [9]:

$$\frac{ds}{dt} = \lim_{x \searrow s(t)} \begin{cases} -h^{m-1} \frac{\partial h}{\partial x} & \text{if } s'(t) \leq 0, \\ h^n \left( \frac{\partial h}{\partial x} \right)^{-1} & \text{if } s'(t) \geq 0, \end{cases} \tag{1.2}$$

where the spatial derivatives are not well defined as  $x \searrow s(t)$ . The analysis of [5, 9, 19] on weak solutions to the slow diffusion equation (1.1) was restricted to the range  $0 < n < 1$ , in which case the zero solution satisfies (1.1) on the infinite line. The weak formulation of the slow diffusion equation (1.1) was also considered in the range  $1 - m < n \leq 0$  (for  $m > 1$ ) in [18], where existence of weak solutions was proven for the modified equation

$$\frac{\partial h}{\partial t} = \frac{\partial}{\partial x} \left( h^m \frac{\partial h}{\partial x} \right) - h^n \chi_{\{h>0\}}. \tag{1.3}$$

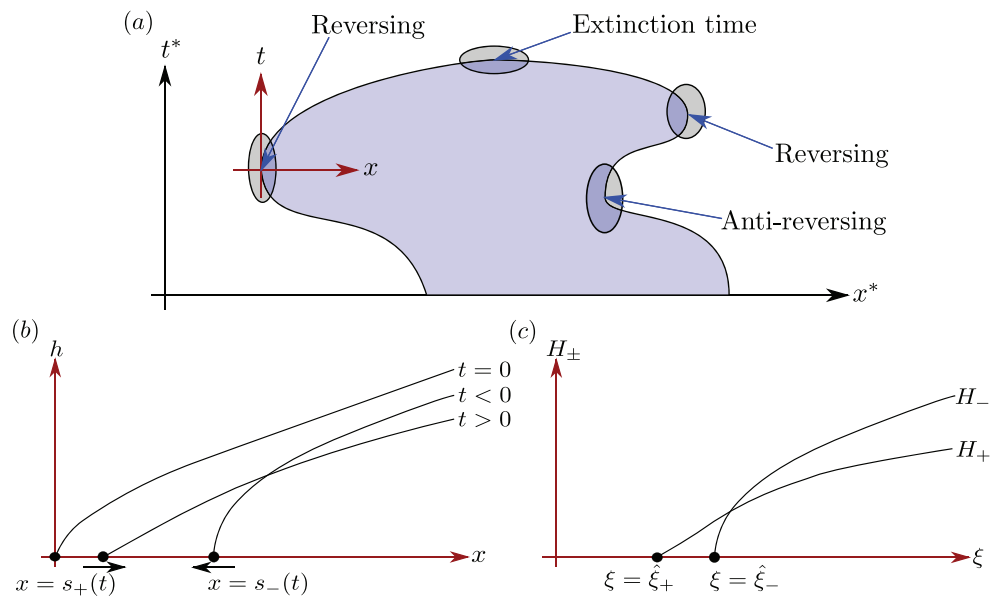


**Figure 1.** Panel (a): schematic scenario of one possible evolution of the compact support (blue region) of a solution to (1.1). Regions in the  $(x^*, t^*)$ -plane corresponding to extinction time, reversing and anti-reversing events are highlighted. Panel (b): possible snapshots of the profile of  $h(x, t)$  (in the local  $(x, t)$ -coordinate system highlighted in red in panel (a)) at three different times local to the reversing event. Panel (c): the corresponding solution profiles  $H_{\pm}$  in the self-similar coordinate system defined in (1.4).

The modification involves the characteristic function  $\chi$  and is included to ensure that the zero solution satisfies (1.3) on the infinite line. Under suitable conditions on the initial data, it was proven in [18] that the weak solutions are classical at the points  $(x, t)$ , for which  $h$  is positive. Hence, the positive solution of the slow diffusion equation (1.3) with  $m > 0$ ,  $n < 1$ , and  $m + n > 1$  can be closed at the left interface  $x = s(t)$  subject to the interface equation (1.2).

A numerical method for time-dependent simulations of the slow diffusion equation (1.3) was developed in section 6 of our previous work [8], where reversing of an interface is observed in numerical simulations with  $n = 0$ . These simulations were compared with the self-similar solutions and it was shown that the reversing event was accurately described by for a variety of different initial data.

We note that conditions (1.2) are not sufficient to close (1.3) on their own. An additional boundary condition is also needed. The boundary condition could be an interface equation at a right interface, or a Dirichlet or Neumann condition elsewhere. However, such details are not important for our purposes because the self-similar solutions that we examine are to be understood in a local sense only (both local to the left interface and local to a reversing event).

After selecting the origin of the spatial and temporal coordinates such that the region of positive  $h$  lies in  $x > 0$  and the reversing or anti-reversing event occurs at  $t = 0$  (at which time the interface is located at  $x = 0$ ), a plausible local behaviour of interfaces is provided by the self-similar solutions in the form suggested in [7],

$$h(x, t) = (\pm t)^{\frac{1}{1-n}} H_{\pm}(\xi), \quad \xi = x(\pm t)^{-\frac{m+1-n}{2(1-n)}} \quad \text{for } \pm t > 0, \quad (1.4)$$

where the functions  $H_{\pm}$  satisfy the following ordinary differential equations (ODEs):

$$\frac{d}{d\xi} \left( H_-^m \frac{dH_-}{d\xi} \right) - \frac{m+1-n}{2(1-n)} \xi \frac{dH_-}{d\xi} = H_-^n - \frac{1}{1-n} H_- \tag{1.5}$$

and

$$\frac{d}{d\xi} \left( H_+^m \frac{dH_+}{d\xi} \right) + \frac{m+1-n}{2(1-n)} \xi \frac{dH_+}{d\xi} = H_+^n + \frac{1}{1-n} H_+. \tag{1.6}$$

It is assumed that  $H_{\pm}$  are positive for  $\xi > \hat{\xi}_{\pm}$ , where  $\hat{\xi}_{\pm}$  are both constants with  $\hat{\xi}_+$  being relevant for  $t > 0$  whilst  $\hat{\xi}_-$  is relevant for  $t < 0$ . Henceforth, we denote the location of the left interface for positive and negative time by  $s_+(t)$  and  $s_-(t)$  respectively. The form of the self-similar solution (1.4) implies that the interface after and before a reversing or anti-reversing event is located at the positions given by

$$s_{\pm}(t) = \hat{\xi}_{\pm} (\pm t)^{\frac{m+1-n}{2(1-n)}}. \tag{1.7}$$

See figure 1 for a sketch of the solutions, including the interface locations, in the various different coordinate systems. Owing to (1.7), in addition to requiring  $m > 0$  and  $n < 1$ , we are also restricted to  $m + n > 1$  so that  $s_{\pm}(t)$  has a physically reasonable behaviour in time with  $\lim_{t \rightarrow \pm 0} s'_{\pm}(t) = 0$ . For technical reasons described below (3.8), we also restrict the range of  $n$  to  $-1 \leq n < 1$ , which includes the most interesting case for many physical applications, namely  $n = 0$ .

The conditions (1.2) and (1.7) imply that solutions to (1.5) and (1.6) are required to satisfy  $H_{\pm} \searrow 0$  as  $\xi \searrow \hat{\xi}_{\pm}$  and

$$\pm \frac{m+1-n}{2(1-n)} \hat{\xi}_{\pm} = \lim_{\xi \searrow \hat{\xi}_{\pm}} \begin{cases} -H_{\pm}^{m-1} \frac{dH_{\pm}}{d\xi} & \text{if } \pm \hat{\xi}_{\pm} < 0, \\ H_{\pm}^n \left( \frac{dH_{\pm}}{d\xi} \right)^{-1} & \text{if } \pm \hat{\xi}_{\pm} > 0. \end{cases} \tag{1.8}$$

For reasons that will become clear shortly the far-field condition

$$H_{\pm} \sim \left( \frac{\xi}{A} \right)^{\frac{2}{m+1-n}} \quad \text{as } \xi \rightarrow +\infty \tag{1.9}$$

completes the specification of the relevant boundary value problems for the system (1.5) and (1.6). The constant  $A > 0$  is determined from solving equation (1.5) and the same  $A$  is taken while solving equation (1.6). Requiring identical far-field behaviours in the solution of both (1.5) and (1.6) is tantamount to ensuring continuity of  $h(x, t)$  across  $t = 0$  with

$$\lim_{t \rightarrow 0} h(x, t) = \left( \frac{x}{A} \right)^{\frac{2}{m+1-n}}. \tag{1.10}$$

Existence of suitable solutions to the boundary-value problem (1.5), (1.6), (1.8) and (1.9) was first suggested in [7]. This was elaborated in [8] with an analytic shooting method that made use of invariant manifold theory for dynamical systems in appropriately rescaled variables near the small and large values of  $H_{\pm}$ . It was also shown in [8] that the self-similar solutions (1.4) are observed in the numerical simulations of the time-dependent problem related to the slow diffusion equation (1.1).

We note the existence of an exact solution to (1.5) and (1.6) in the form

$$H_{\pm}(\xi) = \left( \frac{(m+1-n)^2}{2(m+n+1)} \xi^2 \right)^{\frac{1}{m+1-n}}. \tag{1.11}$$

The conditions (1.8) and (1.9) are satisfied with  $\hat{\xi}_{\pm} = 0$  and  $A = A_Q$ , where

$$A_Q := \left( \frac{2(m+1+n)}{(m+1-n)^2} \right)^{1/2}. \tag{1.12}$$

It is straightforward to verify that in the original spatial and temporal variables given by (1.4) the exact solution (1.11) corresponds to a time-independent solution to the slow diffusion equation (1.1) given by

$$h(x) = \left( \frac{(m+1-n)^2}{2(m+1+n)} x^2 \right)^{\frac{1}{m+1-n}}. \tag{1.13}$$

Hence, the interface is static for the exact solution in (1.11) or (1.13). Although this solution does not constitute a reversing or anti-reversing interface solution, it does play a central role in the bifurcation analysis. Henceforth we refer to (1.11) as the *primary branch* of self-similar solutions to (1.5) and (1.6).

Given that there is a key difference between the boundary-value problems for  $H_-$  and  $H_+$ , namely that  $A$  in (1.9) is found whilst solving for  $H_-$  and then imposed to determine the solution  $H_+$ , we shall provide local analysis of the asymptotic expansions as  $\xi \searrow \hat{\xi}_{\pm}$ . Two types of the leading-order balance may occur here. The first possibility is the usual balance for porous-medium equations, in which the absorption term,  $-h^n$ , is negligible, i.e.

$$\frac{d}{d\xi} \left( H_{\pm}^m \frac{dH_{\pm}}{d\xi} \right) \sim \mp \frac{m+1-n}{2(1-n)} \hat{\xi}_{\pm} \frac{dH_{\pm}}{d\xi}. \tag{1.14}$$

The balance (1.14) is valid for  $\pm \hat{\xi}_{\pm} < 0$  and yields the following local behaviour

$$H_{\pm} \sim \left( \mp \frac{m(m+1-n)\hat{\xi}_{\pm}}{2(1-n)} (\xi - \hat{\xi}_{\pm}) \right)^{1/m} \quad \text{as } \xi \searrow \hat{\xi}_{\pm}. \tag{1.15}$$

The second possibility arises when the diffusion term is negligible, i.e.

$$\pm \frac{m+1-n}{2(1-n)} \hat{\xi}_{\pm} \frac{dH_{\pm}}{d\xi} \sim H_{\pm}^n. \tag{1.16}$$

The balance (1.16) is valid for  $\pm \hat{\xi}_{\pm} > 0$  and yields the following local behaviour

$$H_{\pm}(\xi) \sim \left[ \pm \frac{2(1-n)^2}{(m+1-n)\hat{\xi}_{\pm}} (\xi - \hat{\xi}_{\pm}) \right]^{1/(1-n)} \quad \text{as } \xi \searrow \hat{\xi}_{\pm}. \tag{1.17}$$

The asymptotic behaviours (1.15) and (1.17) were proven rigorously in [8] by using dynamical system methods, and they satisfy the relevant boundary conditions (1.8).

Unlike the ODEs (1.5) and (1.6) and the dominant balance (1.14), the balance (1.16) is of first order and the corresponding local behaviour, (1.17), contains only one degree of freedom, namely  $\pm \hat{\xi}_{\pm}$ . We should therefore check for the presence of a second degree of freedom (in higher order terms) in the usual way by the Liouville–Green (JWKB) method [4], i.e. by linearising the ODEs (1.5) and (1.6) about (1.17). We do so by writing  $H_{\pm} = \hat{H}_{\pm} + \tilde{H}_{\pm}$ , substituting into (1.5) and (1.6) and truncating at terms of  $\mathcal{O}(\tilde{H}_{\pm}^2)$ . On doing so, and on substituting the leading order behaviour (1.17) for  $\hat{H}_{\pm}$ , we derive a second-order linear homogeneous ODE for  $\tilde{H}_{\pm}$  with the following local behaviour

$$\tilde{H}_{\pm}(\xi) \sim \exp\left(\frac{|\hat{\xi}_{\pm}|}{2} \left(\frac{(m+1-n)|\hat{\xi}_{\pm}|}{2(1-n)^2}\right)^{\frac{m}{1-n}} (\xi - \hat{\xi}_{\pm})^{-\frac{m+n-1}{1-n}}\right). \tag{1.18}$$

In the limit  $\xi \searrow \hat{\xi}_{\pm}$  this does not satisfy the requirement that  $|\tilde{H}_{\pm}| \ll |\hat{H}_{\pm}|$ , hence the second degree of freedom is inadmissible. Thus, each of the balances (1.14) and (1.16) contains only one degree of freedom, namely  $\hat{\xi}_{\pm}$ .

As  $\xi \rightarrow +\infty$  the behaviour (1.9) arises from the balance

$$\pm \frac{m+1-n}{2(1-n)} \xi \frac{dH_{\pm}}{d\xi} \sim \pm \frac{1}{1-n} H_{\pm}. \tag{1.19}$$

Since the dominant balance (1.19) is again of first order we employ the Liouville–Green (JWKB) method [4] for a second time to reinstate the second possible degree of freedom that may be contain in the higher order terms of the behaviour (1.9). Carrying out the same linearisation procedure as described above but this time substituting the leading order behaviour (1.9) in place of  $\hat{H}_{\pm}$  we derive a second order linear homogeneous ODE for  $\tilde{H}_{\pm}$  with the following asymptotic behaviour

$$\tilde{H}_{\pm}(\xi) \sim \exp\left(\mp \left(\frac{m+1-n}{2(1-n)} A^{\frac{m}{m+1-n}}\right)^2 \xi^{\frac{2(1-n)}{m+1-n}}\right). \tag{1.20}$$

Here, we find that the requirement  $|\tilde{H}_{\pm}| \ll |\hat{H}_{\pm}|$  in the limit  $\xi \rightarrow +\infty$  is met for the ODE (1.6) whereas it is violated for the ODE (1.5). Thus, the far-field behaviour (1.9) for  $H_-$  contains only a single degree of freedom, namely  $A$ . Again, the behaviour (1.9) was justified in [8] by using dynamical system methods.

In summary, the ODEs (1.5) and (1.6) are to be solved subject to the boundary conditions (1.8) and hence (1.15) or (1.17) as  $\xi \searrow \hat{\xi}_{\pm}$ , where  $\hat{\xi}_{\pm}$  is determined as a part of the solution  $H_{\pm}$ . In terms of the dynamics of the PDE (1.1), the local behaviour of the solutions switches from

$$h(x, t) \sim (-ms'(t)[x - s(t)])^{\frac{1}{m}} \quad \text{with } s'(t) < 0, \tag{1.21}$$

as in (1.15), to

$$h(x, t) \sim \left(\frac{1-n}{s'(t)}[x - s(t)]\right)^{\frac{1}{1-n}} \quad \text{with } s'(t) > 0, \tag{1.22}$$

as in (1.17) at a reversing event, or, vice versa at an anti-reversing event. The parameter  $A$  in the boundary condition (1.9) is determined as a part of the solution  $H_-$  by using a single-parameter shooting from either  $\xi \searrow \hat{\xi}_-$  or  $\xi \rightarrow +\infty$ . Contrastingly, for the purposes of solving for  $H_+$  the value of  $A$  is prescribed to be the same as the one found from the solution  $H_-$ .

A numerical shooting method was developed in [8] for the case  $n = 0$  to connect the near-field and far-field behaviours for (1.5). The connection is possible only for some isolated values of  $A$  denoted by  $A^*$ . This shooting method was used here to obtain a diagram of some possible self-similar solutions in the  $(A, m)$ -plane for few selected values of  $n$ , see figure 2. For each point on the curves depicted there is a unique value of  $\hat{\xi}_-$  which is positive on the red curves (corresponding to a solution that advances for  $t < 0$ ), negative on blue curves (corresponding to a solution that recedes for  $t < 0$ ), and zero on black curves (corresponding to a solution with a static interface for  $t < 0$ ). Figure 3 shows details of the bifurcations in the case

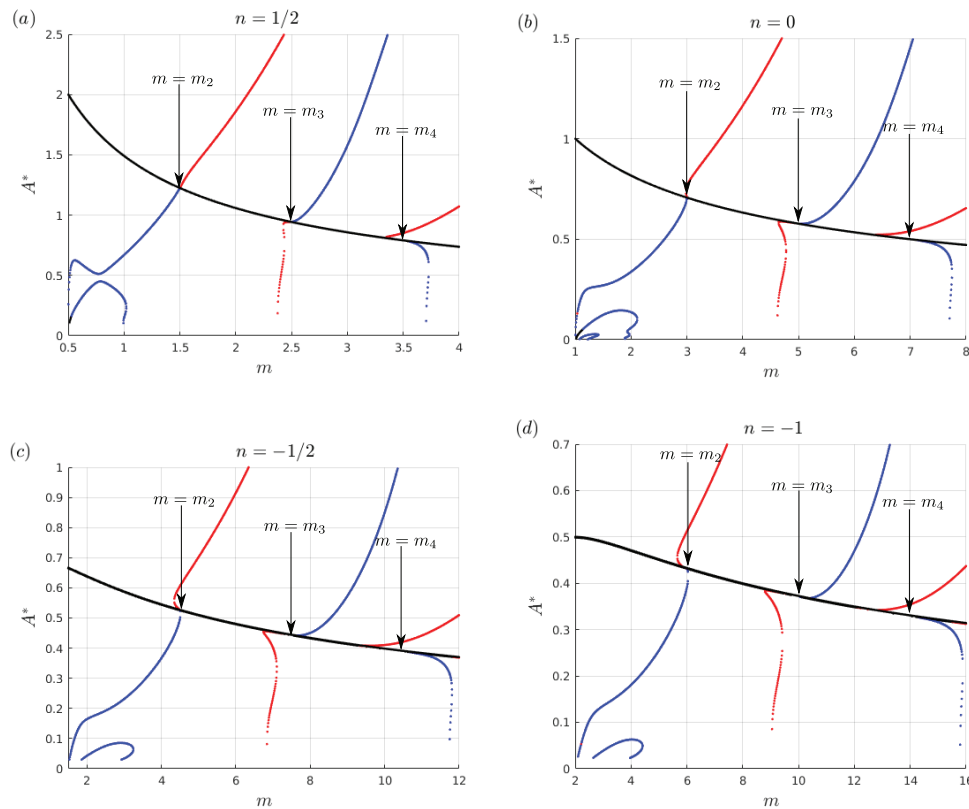


**Figure 2.** The special values of  $A = A^*$  (as a function of  $m$ ) in the behaviour (1.9) that correspond to a solution of the ODE (1.5) with the near field behaviours (1.15) and (1.17). The red, blue and black curves indicate values of  $A^*$  that are associated with solutions with  $\hat{\xi}_- > 0$  (advancing for  $t < 0$ ),  $\hat{\xi}_- < 0$  (receding for  $t < 0$ ), and  $\hat{\xi}_- = 0$  respectively. The values of  $m_2, m_3$ , and  $m_4$  are given in (1.23). Note that solutions with  $A > A_Q$  have  $\hat{\xi}_+ > 0$  whereas those with  $A < A_Q$  have  $\hat{\xi}_+ < 0$ . Thus there is a difference in the physical interpretation between solutions that reside above the black curve to those that reside below it.

$n = 0$ . A short summary of how the plots in figures 2 and 3 were produced is given in section 6 and full details can be found in [8].

Note that the red curves in figure 2 correspond to reversing interfaces only if they are located above the black curves, in which case both  $\hat{\xi}_-$  and  $\hat{\xi}_+$  are positive. However, if the red curves are located below the black curves, then  $\hat{\xi}_- > 0$  and  $\hat{\xi}_+ < 0$ , which corresponds to an advancing interface that instantaneously pauses before continuing its advancing. Similarly, if the blue curves are located below the black curves, they corresponds to the anti-reversing interfaces with  $\hat{\xi}_- < 0$  and  $\hat{\xi}_+ < 0$ . If the blue curves are located above the black curves, then  $\hat{\xi}_- < 0$  and  $\hat{\xi}_+ > 0$ , which corresponds to a receding interface that instantaneously pauses before continuing its receding.

The subtlety explained above (regarding the physical relevance of red and blue curves that lie above/below the black curve in figures 2 and 3) occurs because a valid solution to the ODE (1.6) for  $H_+$  can be obtained for every value of  $A$  in the behaviour (1.9). It was shown in [8]

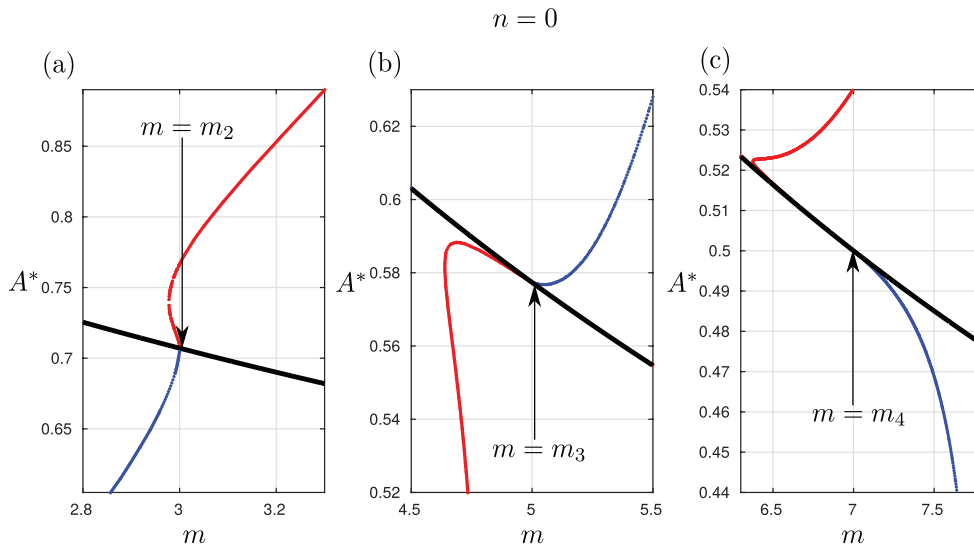


**Figure 3.** Details of the relevant bifurcations for the panel (b) of figure 2 near the bifurcation points  $m_2$ ,  $m_3$  and  $m_4$  given by (1.23).

that  $\hat{\xi}_+$  is a monotonic increasing function of  $A$  with the following properties: if  $A < A_Q$  then  $\hat{\xi}_+ < 0$ , if  $A > A_Q$  then  $\hat{\xi}_+ > 0$  whereas if  $A = A_Q$  then  $\hat{\xi}_+ = 0$ . Thus, if a valid solution to (1.5) can be found, a related solution to (1.6) can always be constructed for the same value of  $A = A^*$ .

The rather exotic patterns visible in figures 2 and 3 depict the existence of bifurcating solutions from the black curve that corresponds to the case  $\hat{\xi}_- = 0$ , and hence to the exact solution (1.11). In particular, we see that bifurcations appear to occur at

$$m = m_k := (2k - 1)(1 - n), \quad k = 2, 3, 4, \dots \tag{1.23}$$

It is natural to conjecture that there is a countable number of bifurcations as  $m$  increases beyond the values shown in figure 2.

The present paper addresses bifurcations of self-similar solutions for reversing and anti-reversing interfaces from the exact solution (1.11). We refer to the bifurcating solutions as the *secondary branches*, which emerge from the primary branch. Since the existence of self-similar solutions is defined by the ODE (1.5), the rest of this work focusses on analysis of this equation only. Although our methods work for every  $-1 \leq n < 1$ ,  $m > 0$ , and  $m + n > 1$ , we will simplify many details by considering the case  $n = 0$  and  $m > 1$ .

Our approach is based on a two-scale asymptotic construction that approximates the bifurcating solutions. Figure 4 shows a representative case where the numerical solution for  $H_-$  (black solid line) is compared with the asymptotic behaviours (1.9) (blue dashed line) and (1.15) (red dashed line). The inner scale captures the local behaviour of the solution  $H_-$  near the interface location  $\hat{\xi}_-$  in the limit when  $\hat{\xi}_-$  is small. The outer scale is used to describe the solution  $H_-$  in the bulk of the semi-infinite line  $(\hat{\xi}_-, \infty)$ . The later solutions rely on the linearization of the ODE (1.5) near the exact solution (1.11), which can be transformed to the classical Kummer’s differential equation [20, 25]. Matching conditions between the two scales can be satisfied when  $m$  is selected near the bifurcation points (1.23).

The paper is organized as follows. The next section, section 2, gives a quick review of properties of Kummer’s differential equation. Then, in section 3 we present linearization of the

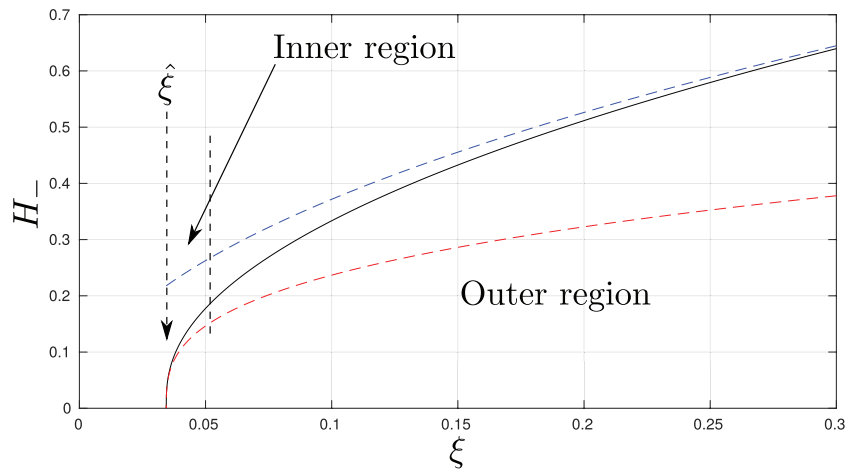


**Figure 4.** The numerical solution  $H_-$  (black solid line) for  $m = 2.99$  and  $n = 0$  with a schematic representation of the two asymptotic scales. The blue dashed line is the far-field behaviour (1.9) and the red dashed line is the near field behaviour (1.15).

ODE (1.5) at the exact solution (1.11). Connection between the linearization and Kummer’s differential equation is reported in section 4. Subsequently, section 5 describes the two-scale asymptotic method that allows us to obtain the secondary branches near the bifurcation points by superposing the bifurcating mode on the primary branch. In section 6 we compare the predictions of the asymptotic method to numerical solutions and observe a good agreement between the two. Finally, section 7 offers physical interpretations of new self-similar solutions obtained in this work.

**2. Kummer’s differential equation**

Here we give a review of some properties of Kummer’s differential equation defined as follows:

$$z \frac{d^2w}{dz^2} + (b - z) \frac{dw}{dz} - aw = 0, \quad z \in \mathbb{R}^+, \tag{2.1}$$

where  $a, b \in \mathbb{R}$  are parameters. Solutions of Kummer’s ODE are confluent hypergeometric functions. We refer the reader to either chapter 13 in [1] or section 9.2 in [13] for a review of confluent hypergeometric functions.

The second-order ODE (2.1) has a regular singular point at  $z = 0$  with two indices

$$\sigma_1 = 0, \quad \sigma_2 = 1 - b,$$

and in what follows we consider  $b > 1$  when  $\sigma_2 < \sigma_1$ . If  $b > 1$ , there exists a unique (up to a multiplicative constant) bounded solution at  $z = 0$  given by the following Kummer’s function [20]

$$M(z; a, b) := 1 + \frac{a}{b} \frac{z}{1!} + \frac{a(a+1)}{b(b+1)} \frac{z^2}{2!} + \frac{a(a+1)(a+2)}{b(b+1)(b+2)} \frac{z^3}{3!} + \dots \tag{2.2}$$

The other singular point of the second-order ODE (2.1) is in the far-field where  $z \rightarrow \infty$  and it is an irregular point with two linearly independent solutions

$$\begin{cases} w_1(z) \sim z^{-a}, \\ w_2(z) \sim z^{a-b}e^z \end{cases} \text{ as } z \rightarrow \infty. \tag{2.3}$$

There exists a unique (up to a multiplicative constant) solution with the algebraic growth at infinity given by the following Tricomi function [25]

$$U(z; a, b) := \frac{\Gamma(1-b)}{\Gamma(1+a-b)}M(z; a, b) + \frac{\Gamma(b-1)}{\Gamma(a)}z^{1-b}M(z; 1+a-b, 2-b), \tag{2.4}$$

such that the function  $U(z; a, b)$  satisfies the asymptotic expansion at infinity (see 13.1.8 in [1]):

$$U(z; a, b) = z^{-a} [1 + \mathcal{O}(|z|^{-1})] \text{ as } z \rightarrow +\infty. \tag{2.5}$$

If  $a$  is not a non-positive integer and  $b > 1$ , then  $U(z; a, b)$  is singular as  $z \rightarrow 0$ :

$$U(z; a, b) = \frac{\Gamma(b-1)}{\Gamma(a)}z^{1-b} [1 + \mathcal{O}(z)] \text{ as } z \rightarrow 0, \tag{2.6}$$

whereas  $M(z; a, b)$  diverges at infinity (see 13.1.4 in [1]):

$$M(z; a, b) = \frac{\Gamma(b)}{\Gamma(a)}z^{a-b}e^z [1 + \mathcal{O}(|z|^{-1})] \text{ as } z \rightarrow +\infty. \tag{2.7}$$

If  $a$  is a non-positive integer, that is, if  $a = -k$  with  $k \in \{0, 1, 2, \dots\}$ , then Kummer’s function  $M(z; a, b)$  is truncated into a polynomial of degree  $k$  so that  $M(z; a, b)$  and  $U(z; a, b)$  are linearly dependent.

Kummer’s differential equation (2.1) is the main ingredient for our analytical method for bifurcations of self-similar solutions. In section 3, we reduce a linearisation of the ODE (1.5) at the exact solution (1.11) to equation (2.1). In section 4, we obtain the connection formulas between  $M(z; a, b)$  and  $U(z; a, b)$  for a non-positive integer  $a$ , which represent the bifurcation points (1.23). These technical details are used in the main part, section 5, where we develop the two-scale asymptotic method for the bifurcating solutions.

### 3. Linearization about the exact solution

In order to interrogate the structure of the bifurcating solutions of the ODE (1.5) local to the primary branch (1.11) we now linearize (1.5) about (1.11). By using the definition (1.12), we can rewrite the exact solution (1.11) in the form:

$$H_Q(r) = r^{\frac{2}{m+1-n}}, \tag{3.1}$$

where  $r := \xi/A_Q$ . By writing  $H_- = H_Q + H$  and dropping terms of  $\mathcal{O}(H^2)$ , we obtain the following homogeneous linear equation for  $H$  valid on  $r > 0$ :

$$\frac{(m+1-n)^2}{2(m+1+n)} \frac{d^2}{dr^2} \left( r^{\frac{2m}{m+1-n}} H \right) - \frac{m+1-n}{2(1-n)} r \frac{dH}{dr} + \frac{1}{1-n} H - nr^{-\frac{2(1-n)}{m+1-n}} H = 0. \tag{3.2}$$

It is necessary to equip the differential equation (3.2) with suitable boundary conditions near the two singular points at  $r = 0$  and as  $r \rightarrow \infty$ . We will show here that there exists two sets of two linearly independent solutions to (3.2) which behave as follows:

$$\begin{cases} H^{(1)}(r) \sim r^{\frac{1+n-m}{m+1-n}}, \\ H^{(2)}(r) \sim r^{\frac{-2(n+m)}{m+1-n}}, \end{cases} \quad \text{as } r \searrow 0 \tag{3.3}$$

and

$$\begin{cases} H^{(I)}(r) \sim r^{\frac{2}{m+1-n}}, \\ H^{(II)}(r) \sim r^{-\frac{3(m+1)-n}{m+1-n}} \exp\left(\frac{m+1+n}{2(1-n)^2} r^{\frac{2(1-n)}{m+1-n}}\right), \end{cases} \quad \text{as } r \rightarrow +\infty. \tag{3.4}$$

In order to justify the asymptotic behaviours (3.3), we use the following transformation of the independent variable

$$y := \frac{m+1-n}{1-n} r^{\frac{1-n}{m+1-n}} \tag{3.5}$$

and rewrite the linear homogeneous equation (3.2) for  $u(y) = H(r)$  in the form

$$\begin{aligned} \frac{(m+1-n)^2}{2(m+1+n)} \left[ \frac{d^2u}{dy^2} + \frac{3m}{(1-n)y} \frac{du}{dy} + \frac{2(m+n)(m-n-1)}{(1-n)^2 y^2} u(y) \right] \\ - \frac{1}{2} y \frac{du}{dy} + \frac{1}{1-n} u(y) = 0, \end{aligned} \tag{3.6}$$

where  $y > 0$ . Use of the Frobenius method (see chapter 4 in [24]) reveals that  $y = 0$  is a regular singular point of the differential equation (3.6) with two indices  $\sigma_{1,2}$  given by the indicial equation

$$\sigma(\sigma - 1) + \frac{3m}{1-n} \sigma + \frac{2(m+n)(m-n-1)}{(1-n)^2} = 0 \tag{3.7}$$

with the two solutions:

$$\sigma_1 = \frac{1+n-m}{1-n}, \quad \sigma_2 = -\frac{2(n+m)}{1-n}. \tag{3.8}$$

We note that  $\sigma_2 < \sigma_1$  for  $m + 3n + 1 > 0$ , which is satisfied if  $m + n > 1$  and  $1 + n \geq 0$ . Therefore, in what follows, we assume that  $-1 \leq n < 1$ .

As follows from the Frobenius method, there exists two linearly independent solutions of the differential equation (3.6) with the following asymptotic behaviours:

$$\begin{cases} u^{(1)}(y) \sim y^{\frac{1+n-m}{1-n}}, \\ u^{(2)}(y) \sim y^{-\frac{2(n+m)}{1-n}}, \end{cases} \quad \text{as } y \searrow 0, \tag{3.9}$$

which justifies (3.3) by the transformation (3.5).

In order to justify the asymptotic behaviours (3.4), we use the following transformation of the dependent variable

$$u(y) = y^{-\frac{3m}{2(1-n)}} \exp\left(\frac{m+1+n}{4(m+1-n)^2} y^2\right) v(y) \tag{3.10}$$

and rewrite the linear homogeneous equation (3.6) in the form

$$-\frac{d^2v}{dy^2} + \left[ \frac{m^2 + 2m + 6mn + 8n^2 + 8n}{4(1-n)^2y^2} - \frac{(3m+5-n)(m+1+n)}{2(1-n)(m+1-n)^2} + \frac{(m+1+n)^2y^2}{4(m+1-n)^4} \right] v(y) = 0. \tag{3.11}$$

The linear equation (3.11) is known in quantum mechanics as the stationary Schrödinger equation for the multi-dimensional harmonic oscillator [22]. Owing to the harmonic confinement of the quantum oscillator, there is only one linear independent solution of the differential equation (3.11) that decays to zero as  $y \rightarrow \infty$ ; the other solution grows rapidly as  $y \rightarrow \infty$ . By using the Liouville–Green (JWKB) method [4], it can be shown that the two linearly independent solutions behave as follows:

$$\begin{cases} v^{(I)}(y) \sim y^{\frac{3m+4}{2(1-n)}} \exp\left(-\frac{m+1+n}{4(m+1-n)^2}y^2\right), \\ v^{(II)}(y) \sim y^{-\frac{3m+6-2n}{2(1-n)}} \exp\left(\frac{m+1+n}{4(m+1-n)^2}y^2\right), \end{cases} \text{ as } y \rightarrow +\infty, \tag{3.12}$$

which justifies (3.4) by the transformations (3.5) and (3.10).

We note that the solution  $H^{(I)}$  in (3.4) matches the asymptotic behavior (1.9), whereas the solution  $H^{(II)}$  grows too fast as  $r \rightarrow \infty$  and must hence be removed. Thus, in agreement with the invariant manifold result of theorem 1.2 in [8], there is a unique (up to a normalizing constant) solution of the linear homogeneous equation (3.2) which satisfies suitable behaviour (1.9) at infinity.

#### 4. Connection between linearization and Kummer’s equation

The stationary Schrödinger equation (3.11) for the multi-dimensional harmonic oscillator is solved in quantum mechanics at the admissible energy levels [22]. These energy levels correspond to the eigenfunctions  $v$  in the function space  $L^2(\mathbb{R}_+)$ . For the function  $H$  satisfying the linear equation (3.2), the admissible energy levels arise from the condition that the algebraically growing solution  $H^{(I)}$  in (3.4) at infinity is connected to the slowest algebraically growing solution  $H^{(1)}$  in (3.3) at zero.

In contrast to a conventional treatment of the stationary Schrödinger equation (3.11), we keep both algebraically growing solutions  $H^{(1)}$  and  $H^{(2)}$  in (3.3) as both play a role in the context of the bifurcating solutions to the ODE (1.5). On the other hand, only the algebraically growing solution  $H^{(I)}$  in (3.4) is allowed by the asymptotic behavior (1.9). Therefore, we only keep one solution  $v^{(I)}$  to the stationary Schrödinger equation (3.11) and continue this solution from infinity to zero. Only the latter solution plays a role for the bifurcating solutions to the ODE (1.5), as we will show in section 5.

In order to construct the solution  $v^{(I)}$  to (3.11), we reduce the stationary Schrödinger equation (3.11) to the Kummer differential equation (2.1). To do so, we use the following transformation of the dependent and independent variables

$$z := \frac{(m+1+n)}{2(m+1-n)}y^2, \quad v(y) := z^{\frac{m+2+2n}{4(1-n)}} \exp\left(-\frac{z}{2}\right) w(z) \tag{4.1}$$

and rewrite the linear homogeneous equation (3.11) in the form

$$z \frac{d^2w}{dz^2} + \left[ \frac{m+3+n}{2(1-n)} - z \right] \frac{dw}{dz} + \frac{m+1-n}{2(1-n)} w(z) = 0, \tag{4.2}$$

which coincides with Kummer's equation (2.1) for

$$a := -\frac{m+1-n}{2(1-n)}, \quad b := \frac{m+3+n}{2(1-n)}. \tag{4.3}$$

Kummer's function  $M(z; a, b)$  defined by (2.2) behaves near zero like the slowest growing solution  $H^{(1)}$  in (3.3) after the transformations (3.5), (3.10) and (4.1) have been used. If  $a$  is not a non-positive integer, then  $M(z; a, b)$  satisfies (2.7), which corresponds to the fastest growing solution  $H^{(II)}$  in (3.4) at infinity. On the other hand, if  $a$  is a non-positive integer, then  $M(z; a, b)$  is truncated into a polynomial, which corresponds to the slowest growing solution  $H^{(I)}$  in (3.4) at infinity. Since the latter is the only one admissible by the asymptotic behaviour (1.9), we record the bifurcation points as follows:

$$a_k := -k, \quad b_k := k + \frac{1+n}{1-n}, \quad k \in \{0, 1, 2, \dots\}, \tag{4.4}$$

in which case,

$$m = m_k := (2k - 1)(1 - n), \quad k \in \{0, 1, 2, \dots\}. \tag{4.5}$$

Note that the bifurcation points given by (4.5) coincide with (1.23) for  $k = 2, 3, 4, \dots$ . Since we are only interested in values of  $m > 0$  and  $n < 1$ , the point at  $m_0 = n - 1 < 0$  can be ignored. We also show in section 5.3.1 that no new branches bifurcate from the point at  $m_1 = 1 - n > 0$ .

Let us state explicitly the polynomials arising at the first four bifurcation points:

$$k = 1 : \quad M(z; a_1, b_1) = 1 - \frac{1-n}{2}z, \tag{4.6}$$

$$k = 2 : \quad M(z; a_2, b_2) = 1 - \frac{2(1-n)}{3-n}z + \frac{(1-n)^2}{2(3-n)(2-n)}z^2, \tag{4.7}$$

$$k = 3 : \quad M(z; a_3, b_3) = 1 - \frac{3(1-n)}{2(2-n)}z + \frac{3(1-n)^2}{2(2-n)(5-3n)}z^2 - \frac{(1-n)^3}{4(2-n)(5-3n)(3-2n)}z^3, \tag{4.8}$$

$$k = 4 : \quad M(z; a_4, b_4) = 1 - \frac{4(1-n)}{5-3n}z + \frac{13(1-n)^2}{(5-3n)(3-2n)}z^2 - \frac{2(1-n)^3}{(5-3n)(3-2n)(7-5n)}z^3 + \frac{(1-n)^4}{4(5-3n)(3-2n)(7-5n)(4-3n)}z^4. \tag{4.9}$$

For every  $a$  and  $b$ , Tricomi's function  $U(z; a, b)$  defined by (2.4) is the only solution of the Kummer's differential equation (2.1) satisfying the asymptotic behaviour (2.5), which corresponds to the slowest growing solution  $H^{(I)}$  in (3.4), after the transformations (3.5), (3.10) and (4.1) have been used. If  $a$  is not a non-positive integer and  $b > 1$ , then  $U(z; a, b)$  satisfies (2.6), which corresponds to the fastest growing solution  $H^{(2)}$  in (3.3). By using (2.6), we define

$$B(m) := \lim_{z \rightarrow 0} z^{b-1}U(z; a, b) = \frac{\Gamma(b-1)}{\Gamma(a)}. \tag{4.10}$$

This quantity determines the fast growth of  $U(z; a, b)$  near  $z = 0$  for  $b > 1$  (which is satisfied in our case under the condition  $m + n > 1$  and  $-1 \leq n < 1$  leading to  $m + 3n + 1 > 0$ ). By using (4.3) and the following continuation formula for the Gamma function (see 8.334 in [13])

$$\Gamma(x)\Gamma(1-x) = \frac{\pi}{\sin \pi x}, \tag{4.11}$$

we compute  $B(m)$  in (4.10) explicitly:

$$\begin{aligned} B(m) &= \frac{\Gamma\left(\frac{m+1+3n}{2(1-n)}\right)}{\Gamma\left(-\frac{m+1-n}{2(1-n)}\right)} \\ &= \pi^{-1}\Gamma\left(\frac{m+1+3n}{2(1-n)}\right)\Gamma\left(\frac{m+3-3n}{2(1-n)}\right)\sin\left(\frac{\pi(m+3-3n)}{2(1-n)}\right). \end{aligned} \tag{4.12}$$

We note that  $B(m_k) = 0$  at the bifurcation point  $m_k$  in (4.5) and

$$B'(m_k) = \frac{1}{2(1-n)}(-1)^{k+1}\Gamma\left(k + \frac{2n}{1-n}\right)\Gamma(k+1). \tag{4.13}$$

In the rest of this section, we compute the limit of  $U(z; a_k, b_k)$  as  $z \rightarrow 0$  for  $a_k, b_k$  given by (4.4) for which  $B(m_k) = 0$ . After the transformations (3.5), (3.10) and (4.1) have been used, this limit of the Tricomi function  $U(z; a_k, b_k)$  corresponds to the slowest growing solution  $\mathbf{H}^{(1)}$  in (3.3) at zero. Hence, we define  $E(m_k) := \lim_{z \rightarrow 0} U(z; a_k, b_k)$  and prove that

$$\begin{aligned} E(m_k) &= (-1)^k \frac{\Gamma(2k+1+p)}{\Gamma(k+1+p)} \\ &= (-1)^k (2k+p)(2k-1+p) \dots (k+1+p), \end{aligned} \tag{4.14}$$

where  $p = 2n/(1-n)$  and we have used  $\Gamma(x+1) = x\Gamma(x)$  for every  $x \in \mathbb{R}$ . In order to justify (4.14), we need to consider both terms in the representation (2.4). The first term has the limit  $z \rightarrow 0$  characterized by the quantity

$$\begin{aligned} C(m_k) &:= \lim_{m \rightarrow m_k} \frac{\Gamma(1-b)}{\Gamma(1+a-b)} = \frac{\Gamma\left(-\frac{m+1+3n}{2(1-n)}\right)}{\Gamma\left(-\frac{m+1-n}{1-n}\right)} \\ &= \lim_{m \rightarrow m_k} \frac{\Gamma\left(\frac{m+2}{1-n}\right)}{\Gamma\left(\frac{m+3+n}{2(1-n)}\right)} \frac{\sin\left(\frac{\pi(m+2)}{1-n}\right)}{\sin\left(\frac{\pi(m+3+n)}{2(1-n)}\right)} \end{aligned} \tag{4.15}$$

where we have used (4.3) and (4.11). With the definition of  $p = 2n/(1-n)$ , we compute the limit  $m \rightarrow m_k$  for  $C(m_k)$  as follows:

$$C(m_k) = \begin{cases} (-1)^k \frac{\Gamma(2k+1+p)}{\Gamma(k+1+p)}, & p \notin \mathbb{Z} \\ 2(-1)^k \frac{(2k+p)!}{(k+p)!}, & p \in \mathbb{Z}, \quad k+p \in \mathbb{N}, \end{cases} \tag{4.16}$$

where we have used  $\Gamma(k+1) = k!$  for  $k \in \mathbb{N}$ . The second term in (2.4) has zero limit  $z \rightarrow 0$  if  $p \notin \mathbb{Z}$  (which ensures that  $b_k - 1$  is not an integer). Therefore, the formula (4.14) is justified from (4.16) with the relation  $E(m_k) = C(m_k)$  if  $p \notin \mathbb{Z}$ .

However, when  $p \in \mathbb{Z}$ , we have

$$z^{1-b_k}M(z; 1+a_k-b_k, 2-b_k) = z^{-k-p}M(z; -2k-p, 1-k-p) \tag{4.17}$$

and since  $-2k - p < 1 - k - p$ , the function (4.17) is not defined if  $1 - k - p$  is a non-positive integer. In order to resolve the singularity, we note the limit 9.214 in [13] for  $k + p \in \mathbb{N}$ :

$$\lim_{b \rightarrow b_k} \frac{M(z; 1 + a - b, 2 - b)}{\Gamma(2 - b)} = \binom{a - 1}{k + p} z^{k+p} M(z; a, b_k). \tag{4.18}$$

By using (4.18), we can first take the limit  $m \rightarrow m_k$  for the second term in (2.4) and then take the limit  $z \rightarrow 0$  to obtain the following contribution for  $b_k - 1 = k + p \in \mathbb{N}$ :

$$\begin{aligned} D(m_k) &:= \lim_{z \rightarrow 0} \lim_{m \rightarrow m_k} \frac{\Gamma(b - 1)\Gamma(2 - b)}{\Gamma(a)} z^{1-b} \frac{M(z; 1 + a - b, 2 - b)}{\Gamma(2 - b)} \\ &= \binom{-1 - k}{k + p} \lim_{z \rightarrow 0} \lim_{m \rightarrow m_k} \frac{\Gamma(1 - a) \sin \pi(1 - a)}{\sin \pi(b - 1)} M(z; a, b), \end{aligned} \tag{4.19}$$

where the continuation formula (4.11) has been used. Since  $M(0; a_k, b_k) = 1$ , further computations yield

$$\begin{aligned} D(m_k) &= (-1)^{k+p} \frac{(2k + p)!}{k!(k + p)!} \lim_{m \rightarrow m_k} \frac{\Gamma\left(\frac{m-3(1-n)}{2(1-n)}\right) \sin\left(\pi\left(\frac{m-3(1-n)}{2(1-n)}\right)\right)}{\sin\left(\pi\left(\frac{m+3n+1}{2(1-n)}\right)\right)} \\ &= (-1)^{k+1} \frac{(2k + p)!}{(k + p)!}. \end{aligned} \tag{4.20}$$

Combining both contributions (4.16) and (4.20) for  $p \in \mathbb{Z}$  together into  $E(m_k) = C(m_k) + D(m_k)$ , we obtain the same expression (4.14) as in the case  $p \notin \mathbb{Z}$ . Thus, the limit  $z \rightarrow 0$  for  $U(z; a_k, b_k)$  given by (4.14) has been justified for every  $p$ .

In section 5, the asymptotic formulas (4.13) and (4.14) are incorporated into the construction of the bifurcating solutions to the ODE (1.5) near the bifurcation point  $m = m_k$ ,  $k \in \mathbb{N}$  given by (4.5).

### 5. Two-scale asymptotic method for bifurcating solutions

Here we consider the differential equation (1.5) with  $n = 0$ , this simplification is made purely to reduce what would otherwise be cumbersome large equations. However, we do note that the cases  $n \neq 0$  with  $-1 \leq n < 1$  can be treated using identical considerations to those outlined below. After the subscript is dropped, the second-order ODE (1.5) with  $n = 0$  is written in the form:

$$\frac{d}{d\xi} \left( H^m \frac{dH}{d\xi} \right) - \frac{m + 1}{2} \xi \frac{dH}{d\xi} = 1 - H. \tag{5.1}$$

We are looking for the monotonically increasing solution on  $[\hat{\xi}, \infty)$  with  $H(\hat{\xi}) = 0$  and

$$-\frac{m + 1}{2} \hat{\xi} = \lim_{\xi \searrow \hat{\xi}} \begin{cases} -H^{m-1} \frac{dH}{d\xi} & \text{if } \hat{\xi} > 0, \\ \left(\frac{dH}{d\xi}\right)^{-1} & \text{if } \hat{\xi} < 0 \end{cases} \tag{5.2}$$

and

$$H(\xi) \sim \left(\frac{\xi}{A}\right)^{\frac{2}{m+1}} \quad \text{as } \xi \rightarrow +\infty, \tag{5.3}$$

for some  $A > 0$ , see (1.8) and (1.9).

As is explained in section 1, there exists an exact solution of equation (5.1)

$$H_Q(\xi) = \left(\frac{\xi}{A_Q}\right)^{\frac{2}{m+1}}, \quad A_Q = \frac{\sqrt{2}}{\sqrt{m+1}}, \tag{5.4}$$

which corresponds to the case  $\hat{\xi} = 0$  in (5.2) and to the case  $A = A_Q$  in (5.3).

Solutions to (5.1) local to the bifurcation values  $m = m_k = 2k - 1$ ,  $k \in \mathbb{N}$  have  $\hat{\xi} \neq 0$  but  $|\hat{\xi}| \ll 1$  in the behaviour (5.2). We therefore seek solutions to (5.1), for  $\xi \gtrsim \hat{\xi}$ , in the asymptotic limit  $\hat{\xi} \rightarrow 0$ . As we will show, taking this limit corresponds to also considering values of  $A$  close to  $A_Q$  in the behaviour (5.3). In this limit solutions are described by two different asymptotic regions, namely: (i) an inner region local to the interface, and (ii) an outer region away from it. See figure 4 for graphical illustration of the two asymptotic regions.

In section 5.1 we detail the structure of solutions close to the interface (the inner region). Then, in section 5.2, we expand solutions of equation (5.1) near the exact solution (5.4) in the bulk (the outer region). The value of  $A$  in the behaviour (5.3) for the asymptotic expansion is defined near  $A_Q$  of the exact solution (5.4). Matching conditions between the two formal asymptotic expansions are considered in section 5.3, where small  $\hat{\xi}$  and  $A - A_Q$  are uniquely defined in terms of  $m - m_k$ . The asymptotic expansions are computed explicitly for  $m_k$  with  $k = 1, 2, 3, 4$ .

5.1. Inner scale

In order to study the behaviour of solutions both in the near field (near the interface at  $\xi = \hat{\xi}$ ), and in the asymptotic limit  $\hat{\xi} \rightarrow 0$  (that is, close to the bifurcation value  $m = m_k$ ), we use the scaling transformation

$$\xi = \hat{\xi} + |\hat{\xi}|^{\frac{m+1}{m-1}} \eta, \quad H(\xi) = |\hat{\xi}|^{\frac{2}{m-1}} \mathcal{H}(\eta), \tag{5.5}$$

where  $\mathcal{H}$  satisfies the second-order ODE for  $\eta > 0$ :

$$\frac{d}{d\eta} \left( \mathcal{H}^m \frac{d\mathcal{H}}{d\eta} \right) = 1 + \frac{m+1}{2} \sigma \frac{d\mathcal{H}}{d\eta} + |\hat{\xi}|^{\frac{2}{m-1}} \left( \frac{m+1}{2} \eta \frac{d\mathcal{H}}{d\eta} - \mathcal{H} \right), \tag{5.6}$$

where  $\sigma = \text{sign}(\hat{\xi})$ . The boundary condition at zero are obtained from (5.2) with  $\mathcal{H}(0) = 0$  and

$$-\frac{m+1}{2} \sigma = \lim_{\eta \searrow 0} \begin{cases} -\mathcal{H}^{m-1} \frac{d\mathcal{H}}{d\eta} & \text{if } \sigma = +1, \\ \left(\frac{d\mathcal{H}}{d\eta}\right)^{-1} & \text{if } \sigma = -1. \end{cases} \tag{5.7}$$

We will study the leading-order term  $\mathcal{H}_0(\eta) = \lim_{\hat{\xi} \rightarrow 0} \mathcal{H}(\eta)$  of the boundary-value problem (5.6)–(5.7). We prove that there exists a unique solution for  $\mathcal{H}_0$  that satisfies

$$\sigma = +1 : \quad \mathcal{H}_0(\eta) \sim \left(\frac{m(m+1)}{2} \eta\right)^{\frac{1}{m}} \quad \text{as } \eta \searrow 0 \tag{5.8}$$

and

$$\sigma = -1 : \quad \mathcal{H}_0(\eta) \sim \frac{2}{m+1} \eta \quad \text{as } \eta \searrow 0. \tag{5.9}$$

These two asymptotic behaviours coincide with (1.15) and (1.17) respectively for  $n = 0$ , after the change of variables (5.5). We also prove that the unique solution for  $\mathcal{H}_0$  satisfies

$$\mathcal{H}_0(\eta) \sim \left(\frac{m+1}{2}\eta^2\right)^{\frac{1}{m+1}} \quad \text{as } \eta \rightarrow +\infty, \tag{5.10}$$

which coincides with the asymptotic behaviour (5.3) for  $A = A_Q$  in (5.4), after the change of variables (5.5).

In the limit  $\hat{\xi} \rightarrow 0$ , the second-order ODE (5.6) is truncated to an autonomous equation for  $\mathcal{H}_0(\eta) = \lim_{\hat{\xi} \rightarrow 0} \mathcal{H}(\eta)$ , which can be integrated once to give

$$\mathcal{H}_0^m \frac{d\mathcal{H}_0}{d\eta} = \eta + \frac{m+1}{2}\sigma\mathcal{H}_0. \tag{5.11}$$

The first-order non-autonomous equation (5.11) is equivalent to the following planar dynamical system

$$\begin{cases} \dot{\eta} = \mathcal{H}_0^m, \\ \dot{\mathcal{H}}_0 = \eta + \frac{m+1}{2}\sigma\mathcal{H}_0, \end{cases} \tag{5.12}$$

where the dot denotes a derivative with respect to the artificial time variable  $\tau$ . The point  $(\eta, \mathcal{H}_0) = (0, 0)$  is the only equilibrium point of the planar system (5.12). If  $m > 1$  (since  $m+n > 1$  and  $n = 0$ ), the equilibrium point  $(0, 0)$  is located at the intersection of a center curve tangential to the straight line

$$E^c(0, 0) = \left\{ \eta = -\frac{m+1}{2}\sigma\mathcal{H}_0, \quad \mathcal{H}_0 \in \mathbb{R} \right\} \tag{5.13}$$

and an unstable (stable) curve for  $\sigma = +1$  ( $\sigma = -1$ ), which is tangential to the  $\mathcal{H}_0$ -axis.

We are only interested in constructing a trajectory of the dynamical system (5.12) in the first quadrant where  $\mathcal{H}_0 > 0$  and  $\eta > 0$ . If  $\sigma = +1$ , the tangent line  $E^c(0,0)$  in (5.13) to the center curve is not located in the first quadrant. Therefore, there is a unique trajectory of the dynamical system (5.12) that departs from  $(0, 0)$  in the first quadrant along the unstable curve and satisfies the exponential growth

$$\mathcal{H}_0(\tau) \sim h_0 \exp\left(\frac{m+1}{2}\tau\right), \quad \eta(\tau) \sim \frac{2h_0^m}{m(m+1)} \exp\left(\frac{m(m+1)}{2}\tau\right) \quad \text{as } \tau \rightarrow -\infty,$$

where  $h_0 > 0$  is an arbitrary constant. Eliminating  $\tau$  yields the asymptotic expression (5.8).

If  $\sigma = -1$ , the tangent line  $E^c(0,0)$  in (5.13) to the center curve is now located in the first quadrant. Since the other invariant curve is stable, there is a unique trajectory of the dynamical system (5.12) that departs from  $(0, 0)$  in the first quadrant along the center curve. The trajectory tangential to  $E^c(0,0)$  satisfies the asymptotic expression (5.9).

If  $\sigma = +1$ , it follows from the first-order equation (5.11) that if a solution originates from the point  $(\eta, \mathcal{H}_0) = (0, 0)$  in the first quadrant, then  $\mathcal{H}_0$  is an monotonically increasing function of  $\eta$  with no stopping points. If  $\sigma = -1$ , the same can be concluded by a contradiction. Suppose there is a finite ‘time’  $\tau_0$  and a finite  $\mathcal{H}_0(\tau_0) > 0$  such that  $\dot{\mathcal{H}}_0(\tau_0) = 0$ . Then, it follows from the system (5.12) that  $\ddot{\mathcal{H}}_0(\tau_0) = \dot{\eta}(\tau_0) = \mathcal{H}_0^m(\tau_0) > 0$ , so that  $\tau_0$  is a minimum of  $\mathcal{H}_0$  as a function of  $\tau_0$ . However, this contradicts the fact that  $\mathcal{H}_0$  was an increasing function of  $\tau$  for  $\tau < \tau_0$ .

Thus, for both  $\sigma = +1$  and  $\sigma = -1$ , the unique solution of the first-order equation (5.11) reaches infinity and since the right-hand side of the second equation in system (5.12) is linear in  $\mathcal{H}_0$ , the solution cannot reach infinity in a finite  $\eta$ . Therefore, the unique solution satisfies  $\mathcal{H}_0 \rightarrow \infty$  as  $\eta \rightarrow \infty$ . In order to derive the asymptotic behavior (5.10), we rewrite (5.11) after another integration with respect to  $\eta$ :

$$\frac{1}{m+1} \mathcal{H}_0^{m+1} = \frac{1}{2} \eta^2 + \frac{m+1}{2} \sigma \int_0^\eta \mathcal{H}_0(\eta') d\eta'. \tag{5.14}$$

It is now easy to justify the asymptotic behaviour (5.10) by iterations.

Summarizing, we have proved the existence of a unique solution to the truncated first-order equation (5.11) which satisfies the leading-order asymptotic expansions (5.8) or (5.9) at zero and the leading-order asymptotic expansion (5.10) at infinity. The behaviour at infinity for the full solution  $\mathcal{H}(\eta)$  is subject to the remainder terms proportional to  $|\hat{\xi}|^{2/(m-1)}$  in the second-order equation (5.6).

We note that the expansion near infinity with the leading-order term in (5.10) is only understood in the asymptotic sense. It was proven in [8] that the trajectory of the differential equation (5.1) that originates at  $H(\hat{\xi}) = 0$  and extends to  $H(\xi) > 0$  for  $\xi > \hat{\xi}$  does not generally reach infinity but turns back towards smaller values of  $H$ . It is only for special values of  $\hat{\xi}$ , that this trajectory reaches infinity to give curves on the solution diagram of figure 2. In order to find these special values of  $\hat{\xi}$ , in the limit of small  $\hat{\xi}$ , i.e. near the bifurcations, we need to construct the outer expansion and to deduce the asymptotic matching conditions on the two-scale expansions.

5.2. Outer scale

Let us consider solutions of the original second-order equation (5.1) in the neighborhood of the exact solution (5.4), which is defined for every  $\xi > 0$ . To do so, we use the following regular asymptotic expansion:

$$H(\xi) = H_Q(r) + \alpha H_1(r) + \alpha^2 H_2(r) + \mathcal{O}(\alpha^3), \quad r := \frac{\xi}{A_Q}, \tag{5.15}$$

where  $\alpha \in \mathbb{R}$  is the small parameter in the formal expansion and the correction terms  $\{H_1, H_2, \dots\}$  are to be defined recursively subject to appropriate boundary conditions. We prove that the first-order correction  $H_1$  satisfies

$$m \neq m_k : H_1(r) \sim B(m) 2^{\frac{m+1}{2}} (m+1)^{-\frac{m+1}{2}} r^{-\frac{2m}{m+1}} \quad \text{as } r \searrow 0, \tag{5.16}$$

and

$$m = m_k : H_1(r) \sim E(m_k) r^{\frac{1-m}{1+m}} \quad \text{as } r \searrow 0 \tag{5.17}$$

where  $B(m)$  and  $E(m_k)$  are given by (4.12) and (4.14) with  $n = 0$ . We also prove that the second-order correction  $H_2$  satisfies

$$m = m_k : H_2(r) \sim F(m_k) r^{-\frac{2m}{m+1}} \quad \text{as } r \rightarrow 0, \tag{5.18}$$

where  $F(m_k)$  is computed from a linear algebraic system. See section 5.3 for details on solutions of this linear system in the cases  $k = 1, 2, 3, 4$ . Note that the dominant term (5.18) in the second-order correction  $H_2$  is comparable with the dominant term (5.16) in the first-order correction  $H_1$  for  $m \neq m_k$ .

In order to justify (5.16)–(5.18), we insert the expansion (5.15) into (5.1) and balance terms at  $\mathcal{O}(\alpha)$  and  $\mathcal{O}(\alpha^2)$ . At  $\mathcal{O}(\alpha)$ , we obtain the homogeneous linear equation

$$\frac{m+1}{2} \frac{d^2}{dr^2} \left( r^{\frac{2m}{m+1}} H_1 \right) - \frac{m+1}{2} r \frac{dH_1}{dr} + H_1 = 0. \tag{5.19}$$

We have proved in section 3 that there is only one solution of the homogeneous equation (5.19) up to a multiplicative factor given by  $\alpha$ , which satisfies the slowest growing behaviour  $H^{(I)}$  in (3.4) as  $r \rightarrow +\infty$ . This solution is given by Tricomi's function  $U(z; a, b)$  in (2.4). After employing the transformations (3.5), (3.10), (4.1) and (4.3) with  $n = 0$ , we can define  $H_1$  in terms of  $r$  as

$$H_1(r) = r^{\frac{1-m}{1+m}} U\left(\frac{m+1}{2} r^{\frac{2}{m+1}}; -\frac{m+1}{2}, \frac{m+3}{2}\right). \tag{5.20}$$

Proceeding to balance terms at  $\mathcal{O}(\alpha^2)$ , we obtain the linear inhomogeneous equation

$$LH_2 = R(H_1), \tag{5.21}$$

where

$$LH_2 := \frac{m+1}{2} \frac{d^2}{dr^2} \left(r^{\frac{2m}{m+1}} H_2\right) - \frac{m+1}{2} r \frac{dH_2}{dr} + H_2 \tag{5.22}$$

and

$$R(H_1) := -\frac{m(m+1)}{4} \frac{d^2}{dr^2} \left[r^{\frac{2(m-1)}{m+1}} H_1^2\right]. \tag{5.23}$$

Owing to the asymptotic behaviour of  $H^{(I)}$  in (3.4) for  $H_1(r)$  as  $r \rightarrow +\infty$ ,  $R(H_1)$  is bounded in the limit  $r \rightarrow +\infty$  and converges to a constant. Since

$$Lr^{\frac{2}{m+1}} = (m+1),$$

there exists a solution  $H_2$  of the inhomogeneous equation (5.21) satisfying the same asymptotic behaviour of  $H^{(I)}$  in (3.4) as  $r \rightarrow +\infty$ . This solution is defined up to the choice of the homogeneous solution proportional to  $H_1$  given by (5.20). Altering this choice of the homogeneous solution simply corresponds to redefining the small parameter  $\alpha$  in the expansion (5.15). Therefore, without loss of generality, the homogeneous solution can be removed from the definition of  $H_2$ , which then becomes uniquely defined.

Now, let us consider the behavior of solutions of the inhomogeneous equation (5.21) near  $r = 0$ . From (4.10) with  $n = 0$ , we know that

$$U(z; a, b) \sim B(m)z^{-\frac{m+1}{2}} \quad \text{as } z \searrow 0,$$

which justifies the asymptotic behaviour (5.16) thanks to the expression (5.20). If  $B(m) \neq 0$ , then  $R(H_1)(r) \sim r^{-4}$  as  $r \searrow 0$ , so that the linear inhomogeneous equation (5.21) produces the solution (up to a multiplicative factor)

$$H_2(r) \sim B(m)r^{-\frac{4m+2}{m+1}}, \quad \text{as } r \searrow 0. \tag{5.24}$$

If  $B(m) = 0$ , the outer expansion (5.15) becomes singular with the fastest growth as  $r \rightarrow 0$ , which cannot be matched with the inner expansion obtained from (5.5) and (5.10). Therefore, we take  $m = m_k$  for some  $k \in \mathbb{N}$ , for which  $B(m_k) = 0$  and rewrite the solution  $H_1$  in the equivalent form:

$$m = m_k : \quad H_1(r) = E(m_k)r^{\frac{1-m}{1+m}} M\left(\frac{m+1}{2} r^{\frac{2}{m+1}}; -k, k+1\right), \tag{5.25}$$

where  $E(m_k)$  is defined by (4.14). This justifies the asymptotic behaviour (5.17). The inhomogeneous term of the linear equation (5.21) is rewritten for  $m = m_k$  in the form:

$$R(H_1)(r) = -\frac{m(m+1)}{4}E(m_k)^2 \frac{d^2}{dr^2} \left[ M^2 \left( \frac{m+1}{2} r^{\frac{2}{m+1}}; -k, k+1 \right) \right]. \tag{5.26}$$

Since  $M(z; -k, k+1)$  is a polynomial of degree  $k$  in  $z$  given by (2.2), the source term contains powers of  $r^{2(-m+\ell)/(m+1)}$  for the integer  $\ell$  counted from 0 to  $m = m_k = 2k - 1$  with the missing factor at  $\ell_k = (m - 1)/2 = k - 1$ . The dominant term  $r^{-2m/(m+1)}$  in  $R(H_1)(r)$  generates the same term in the solution  $H_2(r)$  since

$$Lr^{-\frac{2m}{m+1}} = (m+1)r^{-\frac{2m}{m+1}}.$$

Therefore, in the case  $B(m_k) = 0$ , the linear system of algebraic equations at powers of  $r^{(1-2k+\ell)/k}$  for  $\ell \in \{0, 1, \dots, k-2, k, \dots, 2k-1\}$  is closed. This justifies the asymptotic behaviour (5.18) with some  $F(m_k)$  computed from the linear system.

5.3. Matching conditions

Here we match the two (inner and outer) asymptotic regions together. Using the scaling transformation (5.5) and the leading-order behaviour (5.10), we obtain the dominant term of the inner expansion as follows

$$H(\xi) \sim \left( \frac{\xi - \hat{\xi}}{A_Q} \right)^{\frac{2}{m+1}} \quad \text{as} \quad \frac{\xi - \hat{\xi}}{|\hat{\xi}|^{\frac{m+1}{m+1}}} \rightarrow \infty \quad \text{and} \quad \hat{\xi} \rightarrow 0. \tag{5.27}$$

Expanding as  $\hat{\xi} \rightarrow 0$  and using  $r = \xi/A_Q$ , we obtain

$$H(\xi) \sim r^{\frac{2}{m+1}} - \frac{2\hat{\xi}}{(m+1)A_Q} r^{\frac{1-m}{1+m}} + \frac{(1-m)\hat{\xi}^2}{2(m+1)} r^{-\frac{2m}{m+1}}. \tag{5.28}$$

We can see that the first two correction terms in (5.28) occur also in the first two perturbation terms of the outer expansion (5.15) seen in (5.16)–(5.18). This suggests that two constraints should arise from the matching process. The first constraint on the slowest growing term defines the parameter  $\alpha$  in terms of  $\hat{\xi}$ :

$$-\frac{2\hat{\xi}}{(m+1)A_Q} = \alpha E(m_k) + \mathcal{O}(\alpha(m - m_k), \alpha^2). \tag{5.29}$$

The second constraint on the fastest growing term defines  $m - m_k$  in terms of either  $\alpha$  or  $\hat{\xi}$ :

$$\begin{aligned} \frac{(1-m)\hat{\xi}^2}{2(m+1)} &= \alpha B'(m_k)(m - m_k) 2^{\frac{m+1}{2}} (m+1)^{-\frac{m+1}{2}} + \alpha^2 F(m_k) \\ &+ \mathcal{O}(\alpha(m - m_k)^2, \alpha^2(m - m_k), \alpha^3). \end{aligned} \tag{5.30}$$

After  $\alpha$  is eliminated from the system (5.29) and (5.30), we obtain an asymptotic approximation of the solution curve in the  $(\hat{\xi}, m)$ -plane.

On the other hand, in the limit  $r \rightarrow \infty$ , we compare the outer asymptotic expansion (5.15) with the asymptotic behaviour (5.3) at infinity, where  $A$  is a parameter. From (2.5) and (5.20), we obtain a constraint that defines the parameter  $\alpha$  in terms of  $A - A_Q$ :

$$\left( \frac{A_Q}{A} \right)^{\frac{2}{m+1}} = 1 + \alpha(m+1)^{\frac{m+1}{2}} 2^{-\frac{m+1}{2}} + \mathcal{O}(\alpha^2). \tag{5.31}$$

Equation (5.31) yields the asymptotic approximation of the solution curve in the  $(A, \hat{\xi})$ -plane in view of equation (5.29) or in the  $(A, m)$ -plane in view of the dependence of  $\hat{\xi}$  versus  $m$ .

The sign-alternation of  $E(m_k)$  over  $k \in \mathbb{N}$  given by (4.14) gives rise to (5.29), (5.31) and hence the sign alternation of the dependence  $(A - A_Q)$  versus  $\hat{\xi}$  near the bifurcation point where  $A = A_Q$  and  $\hat{\xi} = 0$ . This fact explains why the location of the red and blue curves bifurcating above and below the black curve on figures 2 and 3 alternates between the two adjacent bifurcation points.

In order to compare our analytical and numerical approaches, let us now compute the asymptotic dependencies near the first four bifurcation points explicitly.

5.3.1. *Behaviour local to  $m = 1$ .* At  $m = 1$ , there exists a one-parameter family of exact solutions to the differential equation (5.1) given by

$$H(\xi) = a(\xi - \hat{\xi}), \quad \hat{\xi} = \frac{a^2 - 1}{a}, \quad a \in \mathbb{R}. \tag{5.32}$$

We show that the matching conditions (5.29)–(5.31) recover the exact solution (5.32). This implies that no new solution branches bifurcate near  $m = 1$ .

On setting  $k = 1$  and  $n = 0$  in (4.13) and (4.14), we obtain  $B'(1) = 1/2$  and  $E(1) = -2$ . Since  $A_Q = 1$ , the matching conditions (5.29) and (5.31) tell us that

$$\hat{\xi} = 2\alpha + \mathcal{O}(\alpha^2), \quad \frac{1}{A} = 1 + \alpha + \mathcal{O}(\alpha^2). \tag{5.33}$$

From (4.6) with  $n = 0$ , (5.25) and (5.26), we obtain  $u_1(r) = r - 2$  and  $R_2(r) = -1$ . From (5.22) with  $m = 1$ , we obtain  $Lr^0 = 1$ . Therefore, there is a unique (up to an addition of the homogeneous solution  $H_1$ ) solution  $u_2(r) = -1$  to the linear equation (5.21), from which we obtain  $F(1) = 0$  in (5.18). The matching condition (5.30) yields

$$m - 1 = \mathcal{O}(\alpha^2). \tag{5.34}$$

Although the approximation (5.34) may imply that  $m \neq 1$  for  $\alpha \neq 0$  (or  $\hat{\xi} \neq 0$ ), let us rewrite the asymptotic solution (5.15) with  $\xi = r$  in the explicit form:

$$H(\xi) = \xi + \alpha(\xi - 2) - \alpha^2 + \mathcal{O}(\alpha^3). \tag{5.35}$$

Comparing (5.35) with the exact solution (5.32) with  $a = 1 + \alpha$  shows that the  $\mathcal{O}(\alpha^3)$  remainder term is identically zero. From (5.3), (5.32) and (5.35), we obtain

$$\hat{\xi} = \alpha \frac{2 + \alpha}{1 + \alpha}, \quad A = \frac{1}{1 + \alpha},$$

which shows that the remainder terms in the second formula (5.33) and in (5.34) are identically zero.

5.3.2. *Behaviour local to  $m = 3$ .* On setting  $k = 2$  and  $n = 0$  in (4.13) and (4.14), we obtain  $B'(3) = -1$  and  $E(3) = 12$ . Since  $A_Q = 1/\sqrt{2}$ , we obtain from (5.29) and (5.31):

$$\hat{\xi} = -12\sqrt{2}\alpha + \mathcal{O}(\alpha^2), \quad \frac{A_Q}{A} = 1 + 8\alpha + \mathcal{O}(\alpha^2),$$

that is,

$$\hat{\xi} = 3(A - A_Q) + \mathcal{O}((A - A_Q)^2). \tag{5.36}$$

In order to use (5.30), we need to compute the coefficient  $F(3)$  in (5.18) from a linear algebraic system. From (4.7) with  $n = 0$ , (5.25) and (5.26), we obtain

$$H_1(r) = 12 \left[ r^{-\frac{1}{2}} - \frac{4}{3} + \frac{1}{3}r^{\frac{1}{2}} \right]$$

and

$$R(H_1)(r) = 12^2 \left[ -2r^{-\frac{3}{2}} + 2r^{-\frac{1}{2}} - \frac{2}{3} \right].$$

From (5.22) with  $m = 3$  we obtain:

$$\begin{aligned} Lr^0 &= 1 + \frac{3}{2}r^{-\frac{1}{2}}, \\ Lr^{-\frac{1}{2}} &= 2r^{-\frac{1}{2}}, \\ Lr^{-\frac{3}{2}} &= 4r^{-\frac{3}{2}}. \end{aligned}$$

Therefore, there is a unique (up to an addition of the homogeneous solution  $H_1$ ) solution to the linear equation (5.21) in the form

$$H_2(r) = 12^2 \left[ -\frac{1}{2}r^{-\frac{3}{2}} + \frac{3}{2}r^{-\frac{1}{2}} - \frac{2}{3} \right],$$

from which  $F(3) = -72$ . The matching condition (5.30) yields

$$-\frac{1}{4}\hat{\xi}^2 = \frac{1}{4}\alpha(3 - m) - 72\alpha^2 + \mathcal{O}(\alpha(3 - m)^2, \alpha^2(3 - m), \alpha^3).$$

Substituting  $\hat{\xi} = -12\sqrt{2}\alpha + \mathcal{O}(\alpha^2)$ , we obtain

$$3 - m = \mathcal{O}(\hat{\xi}^2). \tag{5.37}$$

Although the approximation (5.37) is not definite due to the cancellation of the linear term in  $\hat{\xi}$ , we will show numerically in section 6 that the dependence of  $3 - m$  is indeed quadratic with respect to  $\hat{\xi}$ , see figure 5(a). The precise constant of this quadratic dependence can only be computed if the outer expansion (5.15) is expanded to next order  $\mathcal{O}(\alpha^3)$ , which is not computed here. We also see on figure 5(b) that the approximation (5.36) agrees well with the numerical results.

5.3.3. *Behaviour local to  $m = 5$ .* On setting  $k = 3$  and  $n = 0$  in (4.13) and (4.14), we obtain  $B'(5) = 6$  and  $E(5) = -120$ . Since  $A_Q = 1/\sqrt{3}$ , we obtain from (5.29) and (5.31):

$$\hat{\xi} = 120\sqrt{3}\alpha + \mathcal{O}(\alpha^2), \quad \frac{A_Q}{A} = 1 + 81\alpha + \mathcal{O}(\alpha^2),$$

that is,

$$\hat{\xi} = -\frac{40}{9}(A - A_Q) + \mathcal{O}((A - A_Q)^2). \tag{5.38}$$

The coefficient  $F(5)$  in (5.18) is computed from a linear algebraic system. From (4.8) with  $n = 0$ , (5.25) and (5.26), we obtain

$$H_1(r) = -120 \left[ r^{-\frac{2}{3}} - \frac{9}{4}r^{-\frac{1}{3}} + \frac{27}{20} - \frac{9}{40}r^{\frac{1}{3}} \right]$$

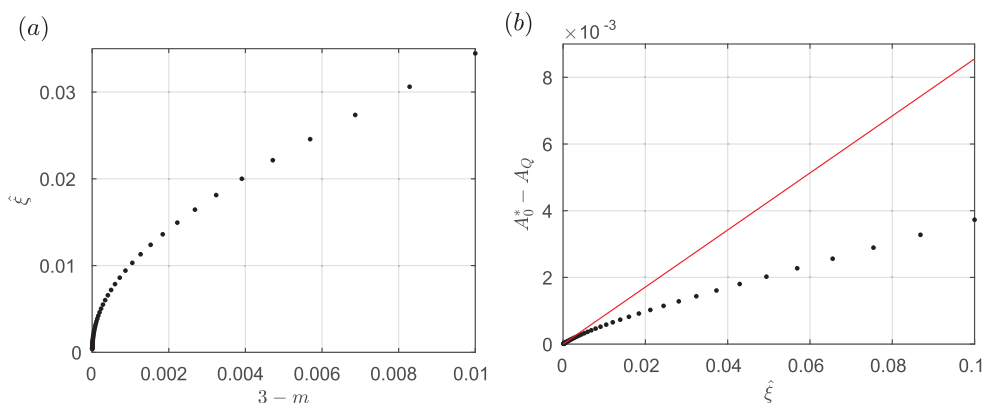


**Figure 5.** Panel (a): the variation of  $\hat{\xi}$  versus  $3 - m$  as predicted by shooting. The observed quadratic dependence of  $3 - m$  on  $\hat{\xi}$  is in agreement with (5.37). Panel (b): the variation of  $A - A_Q$  versus  $\hat{\xi}$  local to  $m = 3$  as predicted by both shooting (black dots) and (5.36) (red line).

and

$$R(H_1)(r) = 120^2 \left[ -\frac{15}{2}r^{-\frac{5}{3}} + \frac{207}{16}r^{-\frac{4}{3}} - \frac{189}{20}r^{-\frac{2}{3}} + \frac{81}{16}r^{-\frac{1}{3}} - \frac{243}{320} \right].$$

From (5.22) with  $m = 5$  we obtain:

$$\begin{aligned} Lr^0 &= 1 + \frac{10}{3}r^{-\frac{1}{3}}, \\ Lr^{-\frac{1}{3}} &= 2r^{-\frac{1}{3}} + \frac{4}{3}r^{-\frac{2}{3}}, \\ Lr^{-\frac{2}{3}} &= 3r^{-\frac{2}{3}}, \\ Lr^{-\frac{4}{3}} &= 5r^{-\frac{4}{3}} - \frac{2}{3}r^{-\frac{5}{3}}, \\ Lr^{-\frac{5}{3}} &= 6r^{-\frac{5}{3}}. \end{aligned}$$

Therefore, there is a unique (up to an addition of the homogeneous solution  $H_1$ ) solution to the linear equation (5.21) in the form

$$H_2(r) = 120^2 \left[ -\frac{77}{80}r^{-\frac{5}{3}} + \frac{207}{80}r^{-\frac{4}{3}} - \frac{387}{80}r^{-\frac{2}{3}} + \frac{243}{64}r^{-\frac{1}{3}} - \frac{243}{320} \right],$$

from which  $F(5) = -13\,860$ . The matching condition (5.30) yields

$$-\frac{1}{3}\hat{\xi}^2 = \frac{2}{9}\alpha(m - 5) - 13\,860\alpha^2 + \mathcal{O}(\alpha(m - 5)^2, \alpha^2(m - 5), \alpha^3),$$

from which we obtain

$$5 - m = \frac{27\sqrt{3}}{4}\hat{\xi} + \mathcal{O}(\hat{\xi}^2). \tag{5.39}$$

The asymptotic dependencies (5.38) and (5.39) will be compared with the numerical data in section 6, where we will see the excellent agreement between them, see figures 6(a) and (b).

5.3.4. *Behaviour local to m = 7.* On setting  $k = 4$  and  $n = 0$  in (4.13) and (4.14), we obtain  $B'(7) = -72$  and  $E(7) = 1680$ . Since  $A_Q = 1/2$ , we obtain from (5.29) and (5.31):

$$\hat{\xi} = -3360\alpha + \mathcal{O}(\alpha^2), \quad \frac{A_Q}{A} = 1 + 1024\alpha + \mathcal{O}(\alpha^2),$$

that is,

$$\hat{\xi} = \frac{105}{16}(A - A_Q) + \mathcal{O}((A - A_Q)^2). \tag{5.40}$$

The coefficient  $F(7)$  in (5.18) is computed from a linear algebraic system. From (4.9) with  $n = 0$ , (5.25) and (5.26), we obtain

$$H_1(r) = 1680 \left[ r^{-\frac{3}{4}} - \frac{16}{5}r^{-\frac{2}{4}} + \frac{16}{5}r^{-\frac{1}{4}} - \frac{128}{105} + \frac{16}{105}r^{\frac{1}{4}} \right]$$

and

$$R(H_1)(r) = 1680^2 \left[ -\frac{84}{5}r^{-\frac{7}{4}} + \frac{1456}{25}r^{-\frac{6}{4}} - \frac{1504}{25}r^{-\frac{5}{4}} + \frac{192}{5}r^{-\frac{3}{4}} - \frac{13\,568}{525}r^{-\frac{2}{4}} + \frac{512}{75}r^{-\frac{1}{4}} - \frac{1024}{1575} \right].$$

From (5.22) with  $m = 7$  we obtain:

$$\begin{aligned} Lr^0 &= 1 + \frac{21}{4}r^{-\frac{1}{4}}, \\ Lr^{-\frac{1}{4}} &= 2r^{-\frac{1}{4}} + 3r^{-\frac{2}{4}}, \\ Lr^{-\frac{2}{4}} &= 3r^{-\frac{2}{4}} + \frac{5}{4}r^{-\frac{3}{4}}, \\ Lr^{-\frac{3}{4}} &= 4r^{-\frac{3}{4}}, \\ Lr^{-\frac{5}{4}} &= 6r^{-\frac{5}{4}} - r^{-\frac{6}{4}}, \\ Lr^{-\frac{6}{4}} &= 7r^{-\frac{6}{4}} - \frac{3}{4}r^{-\frac{7}{4}}, \\ Lr^{-\frac{7}{4}} &= 8r^{-\frac{7}{4}}. \end{aligned}$$

Therefore, there is a unique (up to an addition of the homogeneous solution  $H_1$ ) solution to the linear equation (5.21) in the form

$$H_2(r) = 1680^2 \left[ -\frac{509}{350}r^{-\frac{7}{4}} + \frac{3616}{525}r^{-\frac{6}{4}} - \frac{752}{75}r^{-\frac{5}{4}} + \frac{4376}{315}r^{-\frac{3}{4}} - \frac{2898}{211}r^{-\frac{2}{4}} + \frac{128}{25}r^{-\frac{1}{4}} - \frac{1024}{1575} \right],$$

from which  $F(7) = -4104\,576$ . The matching condition (5.30) yields

$$-\frac{3}{8}\hat{\xi}^2 = \frac{9}{32}\alpha(7 - m) - 4104\,576\alpha^2 + \mathcal{O}(\alpha(7 - m)^2, \alpha^2(7 - m), \alpha^3),$$

from which we obtain

$$7 - m = \frac{2048}{15}\hat{\xi} + \mathcal{O}(\hat{\xi}^2). \tag{5.41}$$

The asymptotic dependencies (5.40) and (5.41) will be compared with the numerical data in section 6, where we will see the excellent agreement between them, see figures 7(a) and (b).

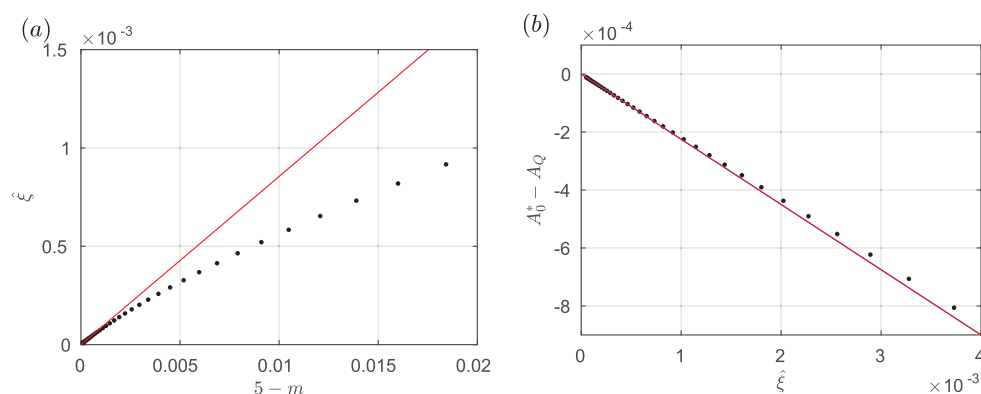


**Figure 6.** Panel (a) shows the variation of  $\hat{\xi}$  versus  $5 - m$  and panel (b) shows the variation of  $A - A_Q$  versus  $\hat{\xi}$  local to  $m = 5$ . Black dots indicate numerical results whereas the red lines in panels (a) and (b) are the behaviours predicted by (5.38) and (5.39) respectively.

### 6. Numerical results

Here we employ numerical methods to verify the analytical results obtained in section 5.3. A fit scheme must be capable of furnishing numerical solutions to the ODE (1.5) which connect the far-field and near-field behaviours given by (1.9) and either (1.15) for  $\hat{\xi}_- > 0$  or (1.17) for  $\hat{\xi}_- < 0$ . Such a numerical method has already been presented in [8] and so in the interests of brevity we will give a short summary—interested readers are referred to [8] for full details.

Finding numerical approximations of solutions for  $H_-$  is a problem that can be tackled using a shooting technique. An appropriate shooting parameter is the value of  $A$  in the far-field behaviour (1.9). On selecting a value for  $A$  the behaviour (1.9) can be used to define approximate initial data for  $H_-(\xi)$  at some very large, yet finite, value of  $\xi$  to begin numerical integration of the ODE (1.5) in the direction of decreasing  $\xi$ . The integration can be continued until either the value of  $H_-(\xi)$  or  $H^m(\xi)H'_-(\xi)$  vanishes at some  $\xi = \hat{\xi}$ ; it was proven in [8] that at least one of these two conditions will be reached for the unique solution satisfying (1.9). The solution to (1.5) we are looking for satisfy both of the aforementioned conditions. It is by iterating on the value of  $A$  that proper solution(s) for  $H_-$  can be found that satisfy both  $H_-(\hat{\xi}_-) = 0$  and  $H^m(\hat{\xi}_-)H'_-(\hat{\xi}_-) = 0$ , for some  $\hat{\xi}_-$ . We denote the special value(s) of  $A$  that give rise to solutions satisfy these conditions by  $A^*$ .

Values of  $A^*$  as a function of  $m$  are shown in figure 2 when the exponent  $n$  of the absorption term in the slow diffusion equation (1.1) is set equal to  $1/2, 0, -1/2, -1$ . From these figures we observe that at each value of  $m = m_k = (2k - 1)(1 - n)$  with  $k = 2, 3, 4, \dots$  two branches of solutions (one with  $\hat{\xi}_- > 0$  (red) and the other with  $\hat{\xi}_- < 0$  (blue)) bifurcate from the main black branch corresponding to the exact solution (1.11) with  $\hat{\xi}_- = 0$ . The bifurcation points were identified in section 4, see (4.5). Moreover, the alternation of the red and blue curves above the black curve between adjacent bifurcations observed on figure 2 can be explained by the sign alternation of  $E(m_k)$  in (4.14) and (5.29) between two values of  $k$ .

The matched asymptotics analysis in section 5 yields prediction of the local dependencies of both  $\hat{\xi}_-$  and  $A^* - A_Q$  on  $m_k - m$  local to each bifurcation point  $m = m_k$  for  $n = 0$ . In figures 5–7 we show a comparison between these predictions and the results of the numerical shooting scheme outlined above. We observe excellent agreement in all cases, thereby

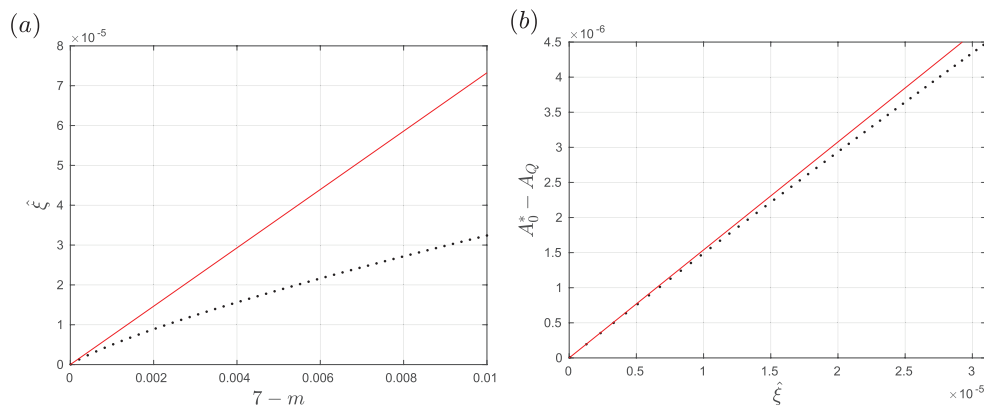


**Figure 7.** Panel (a) shows the variation of  $\hat{\xi}$  versus  $7 - m$  and panel (b) shows the variation of  $A - A_Q$  versus  $\hat{\xi}$  local to  $m = 7$ . Black dots are numerical results whereas the red lines in panels (a) and (b) are the behaviours predicted by (5.40) and (5.41) respectively.

supporting both the analysis presented here and the accuracy of the numerical scheme proposed in [8].

### 7. Conclusion

The work presented here is a contribution towards deepening the understanding of the different types of allowable interface motion in the slow diffusion equation with strong absorption. We have focussed on how an initially advancing interface can give way to a receding one, or vice versa. This work also elucidates the structure of solutions in scenarios where an advancing interface instantaneously pauses and then proceeds to continue its motion in the forward direction, and similarly for a receding interface that pauses and then continues its propagation. Such solutions were identified previously in [7, 8], but the rather complicated structure of the bifurcations of the reversing, anti-reversing and pausing solutions from the stationary branch, see figure 2, were not previously understood. The present paper clarifies the bifurcation structure and demonstrates excellent agreement between the analytical bifurcation results and the numerical approximations of the self-similar solutions.

We conclude by placing the self-similar solutions into the original physical context, i.e. in terms of the PDE (1.1). On transforming to travelling wave-type coordinate system that moves with the position of the left-hand interface (with position  $x = s(t)$ ), using the change of variables  $\eta = x - s(t)$ , and seeking asymptotic solutions to the PDE (1.1) for small values of the moving coordinate,  $\eta$ , we find solutions with local behavior in (1.21) for  $s'(t) < 0$  and in (1.22) for  $s'(t) > 0$ . The local behaviour in (1.21) is termed an advancing interface, since its motion acts to enlarge the domain of compact support, whereas the local behaviour in (1.22) is termed a receding solution. Examining (1.21) we see that the advancing wave is largely controlled by the exponent  $m$  of the diffusive-type term in (1.1). Physically this corresponds to the forward motion of an interface being driven by fluid pressure ( $m = 3$ ), a biological population pressure ( $m = 2$ ) or nonlinear heat conduction ( $m = 4$ ). Contrastingly, the alternative behaviour, (1.22), is controlled by the exponent  $n$  of the absorption term in (1.1). This term corresponds to the physical mechanisms of fluid evaporation or absorption into a substrate or the constant death rate of a biological population ( $n = 0$ ).

A interesting open question concerns the stability of the self-similar reversing, anti-reversing and instantaneously pausing solutions in the time-dependent setting. Although this has been partially addressed in [8] stability for the anti-reversing and pausing solutions remains unknown. Moreover, for pairs of values of  $m$  and  $n$  for which there are more than one solution of a given type, it would be interesting to understand the mechanism that selects the self-similar solution that is observed.

## Acknowledgments

JF was supported by a postdoctoral fellowship at McMaster University. He thanks B Protas for hospitality and many useful discussions. The work of PG was performed within an undergraduate research project in physics at McMaster University. The authors are also grateful to A D Fitt for inspiration and useful discussions.

## ORCID iDs

D E Pelinovsky  <https://orcid.org/0000-0001-5812-440X>

## References

- [1] Abramowitz M and Stegun I A (ed) 1972 *Handbook of Mathematical Functions with Formulas, Graphs, and Mathematical Tables* (New York: Dover)
- [2] Acton J M, Huppert H E and Worster M G 2001 Two dimensional viscous gravity currents flowing over a deep porous medium *J. Fluid Mech.* **440** 359–80
- [3] Aronson D G 1969 Regularity properties of flows through porous media *SIAM J. Appl. Math.* **17** 461–7
- [4] Bender C M and Orszag S A 1999 *Advanced Mathematical Methods for Scientists and Engineers* (New York: Springer)
- [5] Chen X Y, Matano H and Mimura M 1995 Finite-point extinction and continuity of interfaces in a nonlinear diffusion equation with strong absorption *J. Reine Angew. Math.* **459** 1–36
- [6] De Pablo A and Vazquez J L 1990 The balance between strong reaction and slow diffusion *Commun. PDE* **15** 159–83
- [7] Foster J M, Please C P, Fitt A D and Richardson G 2012 The reversing of interfaces in slow diffusion processes with strong absorption *SIAM J. Appl. Math.* **72** 144–62
- [8] Foster J M and Pelinovsky D E 2016 Self-similar solutions for reversing interfaces in the slow diffusion equation with strong absorption *SIAM J. Appl. Dynam. Syst.* **15** 2017–50
- [9] Galaktionov V A, Shmarev S I and Vazquez J L 1999 Regularity of interfaces in diffusion processes under the influence of strong absorption *Arch. Ration. Mech. Anal.* **149** 183–212
- [10] Galaktionov V A, Shmarev S I and Vazquez J L 2000 Behaviour of interfaces in a diffusion-absorption equations with critical exponents *Interfaces Free Boundaries* **2** 425–48
- [11] Galaktionov V A and Vazquez J L 1994 Extinction for a quasilinear heat equation with absorption I. Technique of intersection comparison *Commun. PDE* **19** 1075–106
- [12] Galaktionov V A and Vazquez J L 1994 Extinction for a quasilinear heat equation with absorption II. A dynamical systems approach *Commun. PDE* **19** 1107–37
- [13] Gradshteyn I S and Ryzhik I M 2005 *Table of Integrals, Series and Products* 6th edn (New York: Academic)
- [14] Gurtin M E 1977 On the diffusion of biological populations *Math. Biosci.* **33** 35–49
- [15] Herrero M A and Vazquez J L 1987 The one-dimensional nonlinear heat equation with absorption: regularity of solutions and interfaces *SIAM J. Math. Anal.* **18** 149–67
- [16] Kalashnikov A S 1974 The propagation of disturbances in problems of nonlinear heat conduction with absorption *USSR Comput. Math. Phys.* **14** 70–85

- [17] Kath W L and Cohen D S 1982 Waiting-time behavior in a nonlinear diffusion equation *Stud. Appl. Math.* **67** 79–105
- [18] Kawohl B and Kersner R 1992 On degenerate diffusion with very strong absorption *Math. Methods Appl. Sci.* **15** 469–77
- [19] Kersner R 1983 Nonlinear heat conduction with absorption: space localization and extinction in finite time *SIAM J. Appl. Math.* **43** 1274–85
- [20] Kummer E E 1837 De integralibus quibusdam definitis et seriebus infinitis *J. Reine Angew. Math.* **17** 228–42
- [21] Lacey A A, Ockendon J R and Tayler A B 1982 ‘Waiting-time’ solutions of a nonlinear diffusion equation *SIAM J. Appl. Math.* **42** 1252–64
- [22] Landau L D and Lifschitz E M 1965 *Quantum Mechanics* (Oxford: Pergamon)
- [23] Pritchard D, Woods A W and Hogg A J 2001 On the slow draining of a gravity current moving through a layered permeable medium *J. Fluid Mech.* **444** 23–47
- [24] Teschl G 2012 *Ordinary Differential Equations and Dynamical Systems* (Providence, RI: American Mathematical Society)
- [25] Tricomi F G 1947 Sulle funzioni ipergeometriche confluenti *Ann. Mat. Pura Appl. Quarta* **26** 141–75